The magnetic phase diagram of Ni/Ag antiferromagnetic multilayers

1992 J. Phys.: Condens. Matter 4 4527

(http://iopscience.iop.org/0953-8984/4/18/019)

J. Phys.: Condens. Matter 4 (1992) 4527–4532. Printed in the UK

The magnetic phase diagram of Ni/Ag antiferromagnetic multilayers

B Rodmacq†, B George‡, M Vaezzadeh‡, M Gerl‡ and Ph Mangin‡

† Laboratoire de Métallurgie Physique, SP2M-DRFMC, Centre d'Etudes Nucléaires, 85X, 38041 Grenoble Cédex, France

‡ Laboratoire de Physique du Solide, Université de Nancy I, BP 239, 54506 Vandoeuvre Cédex, France

Received 14 October 1991, in final form 10 February 1992

Abstract. The magnetic phase diagram of antiferromagnetically coupled Ni layers in Ni/Ag superlattices is presented from low temperature up to the ordering temperature. Relations between the neutron scattered intensity (linked to the antiferromagnetic order parameter), the magnetization and the absolute magnetoresistance effect are obtained. The transport properties are observed to be driven by the relative orientations and amplitudes of the magnetizations in successive Ni layers both below and above the ordering line $H^*(T)$.

1. Introduction

The occurrence of antiferromagnetic coupling between thin ferromagnetic films through non-magnetic (or weakly antiferromagnetic) layers [1–7] and the related so-called giant magnetoresistance [8–13] are among the most exciting effects observed in solid state physics during recent years. In several cases [4, 5, 9–12], it has been found that the sign of the coupling is an oscillatory function of the thickness of the non-magnetic layer, with a maximum antiferromagnetic coupling occurring for layer thicknesses close to 10–12 Å.

In these systems, the magnetizations in successive layers are antiparallel in zero field. They tend to align themselves in an external magnetic field and become parallel for a saturation field H_s. At 4.2 K, H_s is typically 20 kOe in the Fe/Cr system [8] and 2 kOe in the Ni/Ag one [6]. The electrical effect related to the rotation of the magnetizations is spectacular. Indeed resistivity drops as large as 80% have been reported [10, 11].

Such behaviour has been qualitatively interpreted via a two-current model in which the cross-section of scattering of the conduction electrons by magnetic atoms depends strongly on the relative orientation between their spin and the atomic moments [8, 14, 15]. Then, when the atomic moments in all layers are aligned, the electrons of one band do not interact much with the magnetic moments and this forms a very highly conducting flow. When the directions of the magnetic moments alternate, the electrons are, whatever their spin, antiparallel to one of the two magnetic sublattices. The two electron currents are thus strongly scattered in every other magnetic layer (or interface), leading to a higher resistivity. Although this qualitative explanation seems to be correct, a lot has still to be done to describe the

0953-8984/92/184527+06$04.50

magnetic behaviour of these systems as a function of applied field and temperature and to determine the relation between the magnetization and resistivity behaviours quantitatively.

In this paper we present a set of magnetization, neutron scattering and magnetoresistance data obtained on a Ni (8 Å)/Ag (11 Å) multilayer. Since samples with Ni layer thicknesses below about 10 Å exhibit ordering temperatures below 300 K [16], this allows one to study the correlation between the magnetization, neutron scattering and magnetoresistance behaviours over the whole temperature range up to the magnetic ordering temperature. These experimental results, plotted in an (H, T) diagram, show that below a particular $H^*(T)$ line, the system exhibits long-range antiferromagnetism and the giant magnetoresistance effect. Above this line, in the absence of antiferromagnetic ordering, the field-induced increase of the magnetization in the layers leads to a further decrease of the electrical resistance.

2. Experimental details

The samples were prepared on glass substrates at 100 K by DC sputtering using deposition rates of the order of 1 Å s^{-1} [17]. Two types of sample were used, thick ones (5 μm) in the form of ribbons 3 mm wide and 20 mm long, onto which platinum wires were spot-welded for resistivity measurements, and thin adherent ones (0.3 μm) with lateral dimensions 15 × 20 mm for neutron experiments. Magnetization measurements were performed on both types of sample to ensure that they were identical, except in thickness. Their structural characteristics have been presented elsewhere [17]. In short, x-ray data showed that the samples were polycrystalline superlattices with (111) textures for both Ag and Ni, with a structural coherence length in the growth direction of about 200 Å.

The magnetization measurements were carried out on a SQUID magnetometer, the field being applied parallel to the plane of the layers. Previous measurements have shown that the easy axis of magnetization lies in the plane whatever the Ni thickness [6]. The magnetoresistance experiments were performed in fields up to 60 kOe with a standard four-probe technique, with both field and current in the plane of the layers. Neutron data were collected on the BT9 instrument at the National Institute of Standards and Technology in Gaithersburg.

3. Results and discussion

The evolution of the magnetization of the sample as a function of the applied field at some selected temperatures is presented in figure 1 on a 0–40 kOe scale. At that scale, the curves can be described as follows: at first the magnetization increases almost linearly up to kink points at $H^*(T)$, $M^*(T)$ with a slope almost independent of the temperature. For $H \geqslant H^*$, the magnetization leaves the 'master curve' and exhibits a subsequent $\Delta M_p(T)$ increase from H^* to 40 kOe. On an expanded scale, from which the values of H^* and M^* were determined, one can see, however, that the master curve is not exactly unique and linear. As seen in figure 1, H^* and M^* tend to zero at a critical temperature T_{cr} = 290 K. Above this temperature, the magnetization leaves the master curve at 0 kOe and there is no sign of ferromagnetism in the Ni layers. The reduced field $h^* = H^*(T)/H^*(0)$ and reduced magnetization

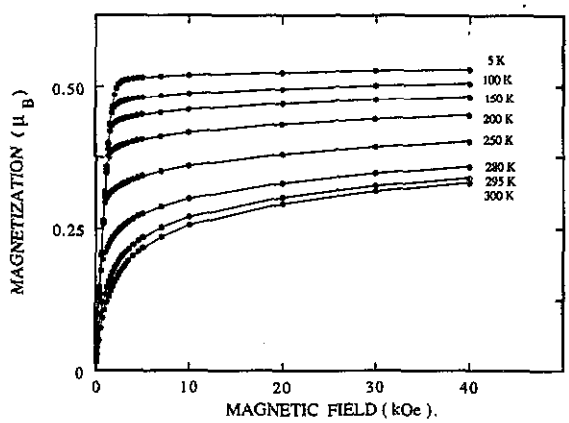

Figure 1. Magnetization curves of a Ni (8 Å)/Ag (11 Å) multilayer at different temperatures.

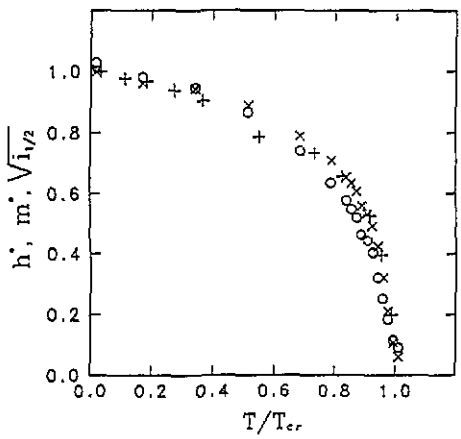

Figure 2. The reduced saturation field h^* (open circles), saturation magnetization m^* (crosses) and square root of the intensity of the antiferromagnetic neutron peak (plus signs) as functions of the reduced temperature.

$m^* = M^*(T)/M^*(0)$ are plotted versus the reduced temperature T/T_{cr} in figure 2. The difference between the reduced-parameter curves is due to the fact that the master curve is not exactly linear.

$M^*(T)$ can be interpreted as the spontaneous magnetization in the Ni layers. At low field, the spontaneous magnetizations of adjacent Ni layers are in the plane of the sample, antiparallel to each other and almost perpendicular to the external field. When the field increases, they progressively rotate towards the field direction. The angle θ between the spontaneous magnetizations in the layers and the field direction varies from 90° for $H = 0$ to 0° for $H = H^*(T)$. Below H^*, this phenomenon can be analysed by minimizing the energy:

$$E = +W(M^*)^2 \cos 2\theta - M^* H t \cos\theta$$

where W is the coupling constant through the non-magnetic layer, H is the applied field and t is the thickness of the magnetic layer. This mean-field type formulation, different from the one presented by other authors [9, 14] where the exchange term is simply written $J \cos 2\theta$, leads to a spin-flop state in which, up to $H = H^*$, the net

magnetization increases linearly with the applied field with a slope $t/4W$. The fact that a master curve is obtained in the present Ag/Ni system (figure 1) implies that the coupling constant W does not depend significantly on the temperature. Above H^*, the magnetization increases because the field reduces the thermal fluctuations of the magnetizations in each Ni layer. Above the ordering temperature, only this contribution remains. The maximum susceptibility (for $H > H^*$) is at T_{cr} where ΔM_p is maximum.

The zero-field neutron scattering pattern exhibits a low-angle 'Bragg peak' due to the chemical modulation at $q_1 = 0.34$ Å^{-1} and a superstructure peak of intensity $I_{1/2}(T)$ at $q_{1/2} = 0.17$ Å^{-1} due to the antiferromagnetic coupling between adjacent ferromagnetic Ni layers. We showed in a previous paper [7] that the intensity of this antiferromagnetic peak measured at 4.2 K decreased with increasing the applied field up to H^*. More precisely the square root of this intensity was found to vary as $m^* \sin\theta$, which is the antiferromagnetic order parameter. The evolution of the square root $\sqrt{i_{1/2}}$ of the normalized intensity $i_{1/2} = I_{1/2}(T)/I_{1/2}(0)$ of the superstructure peak is shown in figure 2. Magnetization and neutron scattering measurements performed on the same sample gave values of the ordering temperature differing by less than 3 K. This difference is not significant. From figure 2, it appears that $\sqrt{i_{1/2}}$ varies as m^* as a function of temperature which, according to the classical relation giving the intensity of the magnetic peaks in antiferromagnets, is in agreement with the intepretation of $M^*(T)$ as the spontaneous magnetization of the two antiferromagnetic sublattices.

A set of curves showing the evolution of the magnetoresistance ratio with applied field at different temperatures is presented in figures 3 and 4 at two different scales. For every temperature below T_{cr}, the resistance first drops rapidly from $R_0(T)$ at $H = 0$ to $R^*(T)$ at a field that is found to be very close to $H^*(T)$ obtained from magnetization measurements. Since the resistivity is lower when the spins in successive layers are parallel, this drop corresponds to the progressive rotation of the spontaneous magnetizations in the layers towards the direction of the applied field [18, 19]. Beyond $H^*(T)$ a subsequent slow decrease of the resistance $\Delta R_p(T)$ is observed (figure 4). It is related to a reduction of the thermal fluctuations leading to a statistically better alignment of the magnetic moments in each layer, and as a consequence between successive layers also. Above T_{cr} only this slow resistance decrease remains. This behaviour is to be related to that of the magnetization above H^*.

More quantitatively, let us call $\Delta R(H) = R(0) - R(H)$ the absolute resistance difference between zero field and any field H below or above H^*. This quantity is plotted in figure 5 versus the square of the magnetization for several temperatures. Figure 5 shows that a linear relationship holds between $\Delta R(H)$ and $M^2(H)$, although some deviation can be noted above H^* (marked by an arrow in the figure). Moreover the slope obtained appears to be independent of the temperature. Such linear behaviour is consistent with a decrease of the resistivity proportional to the cosine of the angle between the magnetic moments by which the conduction electrons are successively scattered [18].

From figure 5, it is clear that the three sets of data—magnetization, neutron scattering and magnetoresistance—are correlated. Below T_{cr} and $H^*(T)$, one observes a neutron antiferromagnetic peak, the resistance scales with the square of the magnetization, and thus varies in a parabolic way with the applied field (figure 3). Above T_{cr} or $H^*(T)$, there is no more antiferromagnetic long-range order (no neutron peak),

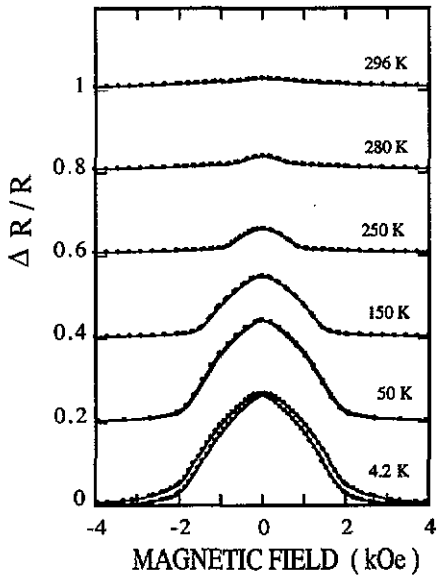

Figure 3. The magnetoresistance ratio as a function of the applied field at different temperatures.

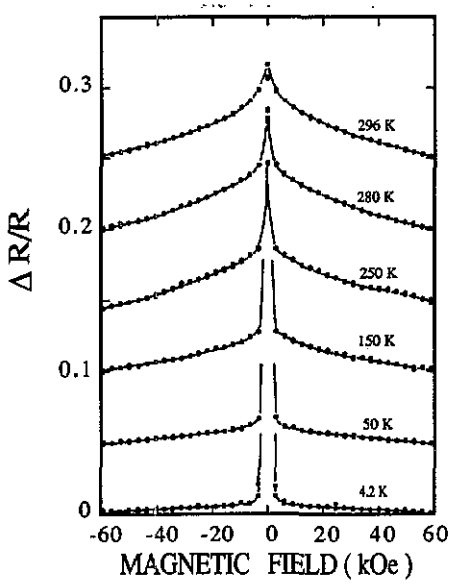

Figure 4. As figure 3, but on different field and resistivity scales.

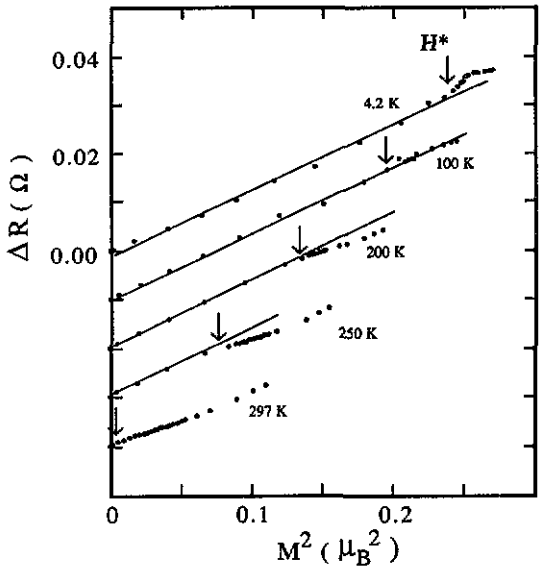

Figure 5. The absolute resistance difference versus the square of the magnetization. The curves have been shifted vertically for clarity. The arrow on each curve gives the position of H^*.

but the magnetization and resistance still vary in the same way with the applied field. In addition, the fact that identical slopes are obtained at different temperatures implies that $\sqrt{\Delta R(T)}$ follows the same thermal variation as m^* and $\sqrt{i_{1/2}}$ (depicted in figure 2). Thus it appears that all these physical quantities depend mainly on the relative alignment of the magnetizations in adjacent magnetic layers, even when there

is no antiferromagnetic long-range order [18]. In that case this alignment can be changed by the applied field or the temperature.

4. Conclusion

We have presented in this paper a study of the field and temperature dependences of the magnetic structure in Ag/Ni superlattices. Two phenomena have been observed: the rotation (below T_{cr}) of the spontaneous magnetizations of the Ni layers up to H^*, followed by the decrease of the thermal fluctuations under the effect of the magnetic field. Both lead to a better alignment of the magnetic moments in adjacent Ni layers and, as a consequence, to a decrease of the electrical resistivity. These results give evidence of a correlation between magnetization, antiferromagnetic neutron intensity and absolute magnetoresistance as a function of both applied field and temperature. Finally, $H^*(T)$ is the transition line separating the region where the antiferromagnetic order parameter is not zero (classically called spin-flop when the magnetic moments are first perpendicular and then aligned in the external field) from the region that is called paramagnetic in metamagnetic systems [20]. No line separates the points for which $T > T_{cr}$ from those for which $T < T_{cr}$ and $H > H^*$.

Acknowledgments

The authors would like to thank the NIST for allocation of beam time and R W Erwin for his help in the neutron experiments.

References

[1] Grünberg P, Schreiber R, Pang Y, Brodsky M B and Sowers H 1986 *Phys. Rev. Lett.* **57** 2442
[2] Cebollada A, Martinez J L, Gallego J M, de Miguel J J, Miranda R, Ferrer S, Batallan F, Fillion G and Rebouillat J P 1989 *Phys. Rev.* B **39** 9726
[3] Pescia D, Kerkmann D, Schumann F and Gudat W 1990 *Z. Phys.* B **78** 475
[4] Bennett W R, Schwarzacher W and Egelhoff W F Jr 1990 *Phys. Rev. Lett.* **65** 3169
[5] Unguris J, Celotta R J and Pierce D T 1991 *Phys. Rev. Lett.* **67** 140
[6] Dos Santos C A, Rodmacq B, Vaezzadeh M and George B 1991 *Appl. Phys. Lett.* **59** 126
[7] Rodmacq B, Mangin Ph and Vettier Chr 1991 *Europhys. Lett.* **15** 503
[8] Baibich M N, Broto J M, Fert A, Nguyen Van Dau F, Petroff F, Etienne P, Cruezet G, Friederich A and Chazelas J 1988 *Phys. Rev. Lett.* **61** 2472
[9] Parkin S S P, More N and Roche K P 1990 *Phys. Rev. Lett.* **64** 2304
[10] Mosca D H, Petroff F, Fert A, Schroeder P A, Pratt W P Jr and Loloee R 1991 *J. Magn. Magn. Mater.* **94** L1
[11] Parkin S S P, Bhadra R and Roche K P 1991 *Phys. Rev. Lett.* **66** 2152
[12] Araki S, Yasui K and Narumiya Y 1991 *J. Phys. Soc. Japan* **60** 2827
[13] Pratt W P Jr, Lee S-F, Slaughter J M, Loloee R, Schroeder P A and Bass J 1991 *Phys. Rev. Lett.* **66** 3060
[14] Barthélémy A, Fert A, Baibich M N, Hadjoudj S, Petroff F, Etienne P, Cabanel R, Lequien S, Nguyen Van Dau F and Creuzet G 1990 *J. Appl. Phys.* **67** 5908
[15] Wang Y, Levy P M and Fry J L 1990 *Phys. Rev. Lett.* **65** 2732
[16] Rodmacq B and Dos Santos C A 1992 *Proc. Int. Conf. on Magnetism (Edinburgh, 1991): J. Magn. Magn. Mater.* **104–7** 1739
[17] Rodmacq B 1991 *J. Appl. Phys.* **70** 4194
[18] Dieny B, Speriosu V S, Parkin S S P, Gurney B A, Wilhoit D R and Mauri D 1991 *Phys. Rev.* B **43** 1297
[19] Chaiken A, Prinz G A and Krebs J J 1990 *J. Appl. Phys.* **67** 4892
[20] Stryjewski E and Giordano N 1977 *Adv. Phys.* **26** 487